The analysis of the association between neuroinflammation and alpha−synuclein propagation in Parkinson's disease

파킨슨병에서 알파시누클레인 병리 진행과 신경염증반응의 관계

2021년 8월

서울대학교 대학원

의학과 뇌신경과학 전공

김 영 은

The analysis of the association between neuroinflammation and alpha−synuclein propagation in Parkinson's disease

지도 교수 전 범 석

이 논문을 의학박사 학위논문으로 제출함

2021년 7월

서울대학교 대학원

의학과 뇌신경과학 전공

김 영 은

김영은의 의학박사 학위논문을 인준함

2021년 7월

위 원 장 ＿＿＿＿＿＿＿＿＿＿

부위원장 ＿＿＿＿＿＿＿＿＿＿

위 　 원 ＿＿＿＿＿＿＿＿＿＿

위 　 원 ＿＿＿＿＿＿＿＿＿＿

위 　 원 ＿＿＿＿＿＿＿＿＿＿

초   록

알파시누클레인 (alpha-synuclein[αSyn]) 단백의 비정상적인 응집과 축적은 파킨슨병의 중요한 병리기전으로 알려져 있다. 또한, 최근 수년 간 신경염증(neuroinflammation)이 파킨슨병의 위험도를 높이고, 병인 에 기여한다는 것이 여러 연구들을 통해 알려지고 있다. 그러나, 이런 알파시누클레인 단백 병리의 진행과 신경염증의 상관관계에 대해서는 알 려진 것이 많지 않다. 이 연구에서는 병적인 형태의 알파시누클레인 단 백(αSyn preformed fibril [PFF])을 직접 생쥐의 뇌에 주사하여, 알파 시누클레인 병리 진행과 신경염증반응의 상관 관계를 규명하고자 한다. 이 연구를 통해, 병적 알파시누클레인을 주사하면, 신경염증 반응 중 특 히 신경아교세포(microglia)의 활성화가 별아교세포(astrocyte) 관련 염증보다 훨씬 많이 증가하는 것을 발견하였다. 또한 병적인 알파시누클 레인 단백을 주입하면, 신경염증반응이 제일 먼저 발생하고, 알파시누클 레인 단백 생성이 증가하며, 병적인 알파시누클레인의 세포내 축적은 그 이후 나타나고, 마지막으로 신경세포 사멸이 나타나는 것을 발견하였다. 이 연구를 근거로 내독소(endotoxin, lipopolysaccharides)로 염증반응 을 증가시키면 알파시누클레인 응집과 축적이 더 많이 증가하고, 반대로 신경아교세포를 억제 시키면 알파시누클레인의 응집과 축적이 감소하였 다. 이 연구를 통해 알게 된 알파시누클레인 병리와 신경염증 반응의 시 간적 연관성 및 알파시누클레인 병인에 좀 더 기여하는 신경염증반응의 종류를 증명하였으며, 이 염증반응의 억제가 알파시누클레인 병리 진행 을 감소시키는 것을 알게 되었다. 이는 파킨슨병의 병인을 이해하고 치 료제 개발에 도움이 될 것이다. 또한 이후 이런 상관관계에 대한 좀 더 자세한 분자 경로 연구가 필요할 것으로 생각된다.

주요어: 알파시누클레인, 신경염증, 신경아교세포, 별아교세포, 파킨슨병, 신경퇴행

학   번: 2012-30541

Table of Contents

3.3 Study 3

Chapter 1. Introduction

1.1. Study Background

Parkinson's disease (PD), the second most common neurodegenerative disease, is characterized by a profound loss of nigrostriatal dopaminergic neurons. Its relevant clinical features include parkinsonism–bradykinesia, rigidity, gait disturbance, and tremor.[1] Intraneuronal inclusions stained with alpha-synuclein (αSyn) antibody, Lewy bodies and Lewy neurites, are regarded as the pathologic hallmark of PD.[2] With recent evidences, αSyn aggregation and accumulation may be involved in both the pathology and pathophysiology of PD. The Mutation of gene encoding α Syn protein such as duplication, triplication and aggregation prone mutation cause PD, and the cell-to-cell transmission of αSyn was evidenced in the transplanted cells of a fetal nigral cell-transplanted PD brain.[3, 4] In addition, the injection of fibrillar αSyn into an animal brain induced a widespread αSyn accumulation and propagation.[5] Therefore, the abnormal aggregation, accumulation, and propagation of the αSyn protein in the nervous system may be considered as a contributing disease mechanism of PD.[5] Other mechanisms, including neuroinflammation, autophagy-lysosomal dysfunction, and oxidative stress, are also involved in the pathophysiology of PD.

Neuroinflammation is one of the important mechanisms contributing to the pathogenesis of PD in recent years. Recent epidemiologic studies reported that various autoimmune diseases are associated with an increased risk of PD. [6-8] In addition, it was reported that the use of anti-inflammatory drugs decreases the risk of PD.[9-11] Genetic studies have supported this association of PD and immune system, stating that several HLA gene loci encoding for MHC class II are associated with a risk for PD.[12] In a postmortem PD brain, microgliosis was reported in various brain regions, including the substantia nigra (SN), while astrogliosis has been described in various levels.[13] In addition to microglial and astrocytic activation in a PD brain, an increased expression of markers, such as MHC-II and MHC-I, and T-cell infiltration into the brain parenchyma have also been reported.[14] Although many evidences

suggested that neuroinflammation and αSyn propagation are associated with the pathophysiology of PD, their relationship remains unclear.

In a recent study, the autopsy data from fetal nigral cell grafting into the brain of a patient with PD showed that both microglial activation and αSyn accumulation were observed, and microglial activation preceded αSyn accumulation in the transplanted young cells.[15] Although the specific role of inflammation in this αSyn-associated disease process is not fully understood, inflammation may not just be a result of the disease process but also a contributor to the progressive nature of synucleinopathy. Additionally, microglia and astrocytes, as innate immune cells in the central nervous system (CNS), may play a different or shared role in PD pathogenesis. However, the relationship between inflammation and αSyn propagation is still not well understood.

The evaluation of a postmortem human brain is the resultant findings of all disease processes and reflects an advanced disease state; therefore, it could not discriminate the temporal or causal relationships between different mechanisms. In addition, previous animal models were based on toxin-induced or transgenic mechanisms, which cannot reflect the spontaneous αSyn propagation process. In recent years, an artificially made αSyn preformed fibril (PFF)-injected animal model has been noted to mimic the αSyn propagation hypothesis, and this model may be valuable in studying the relationship between αSyn spreading and neuroinflammation. Taking advantage of this animal model, we planned to evaluate the association between αSyn propagation and inflammation.

In this study, the recognition of the temporal relationship between inflammation and αSyn propagation and the differential inflammatory cell responses regarding αSyn propagation may be helpful to understand the relationship between the two proposed mechanisms. Then, based on this, we evaluated whether an increased inflammation contributes to αSyn propagation and whether blocking this inflammatory process reduces the αSyn propagation.

1.2. Purpose of Research

This study aimed to determine the relationship between the inflammatory response and αSyn propagation in PD.

In first two parts, we evaluated the differential response of two innate immune cells in the CNS, microglia and astrocytes, on αSyn propagation and the temporal relationship of inflammatory response and αSyn propagation in a mouse model injected with fibrillar αSyn. The first study was the comparison of the two main inflammatory responses (microglia and astrocytes) after the injection of fibrillar αSyn into the mouse brain. It was hypothesized that the innate immunity of the CNS by the resident microglia and astrocytes will respond differently on αSyn propagation. The second study was the analysis of the temporal change in inflammatory response, αSyn propagation, and neurodegeneration in a fibrillar αSyn-injected PD mouse model. It was assumed that the pathological αSyn propagation may be associated with inflammation, and those pathological processes may have temporal relationship.

Finally, in third study, based on the results of the two preceding studies, we evaluated whether an artificially increased inflammation contributes to αSyn propagation and in reverse, we tested whether blocking the inflammatory process reduces the αSyn propagation.

Chapter 2. Study schematics and methods

2.1. Study Schematics

Figure 1. Study schematic
#1 is the plan for study 1, and #2 is the plan for study 2

Study schematic: The analysis of association between inflammation and αSyn propagation
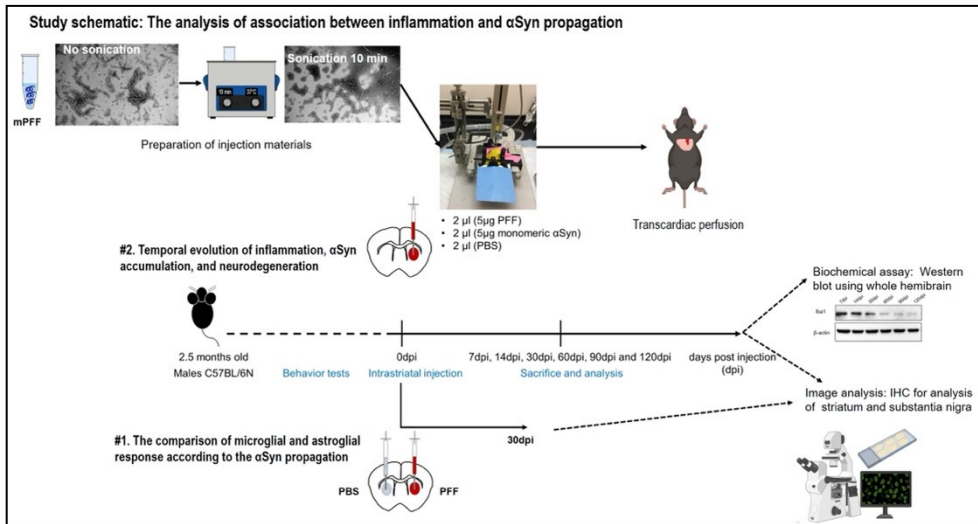
2.1.1 Study 1

The comparison of the two main inflammatory cells (microglia and astrocytes) after injection of fibrillar αSyn into the mouse brain. Figure 1 shows the study scheme for this purpose. One month after the injection of αSyn PFF in one side of the striatum and control substance (phosphate buffered saline [PBS]) to the other striatum, the mouse brain was sacrificed. Using a serially sectioned mouse brain, the αSyn propagation, astrocytes, and microglia were evaluated by immunohistochemistry in the level of the striatum and SN. From the images taken by confocal microscopy, the microglial and astrocytic activation were analyzed based on the distance from the substance injection site in each striatum. The inflammatory response in the SN was also evaluated.

2.1.2. Study 2.

The temporal change in inflammation, αSyn propagation, and neurodegeneration in αSyn PFF-injected PD mouse model was analyzed. This study scheme is shown in Figure 1, #2. αSyn PFF was injected into one side of the striatum of mice. To evaluate the longitudinal pattern of αSyn spreading, inflammation, and neurodegeneration in the PD mouse model, the mice were sacrificed at different time points, including at baseline without injection (0-day post-injection, 0 dpi), 7 dpi, 14 dpi, 30 dpi, 60 dpi, 90 dpi, and 120 dpi. Using the serial brain sections of the striatum,

immunohistochemistry identified the changes in dopaminergic neuron, αSyn accumulation, microglia, and astrocytes. Using the whole brain lysates (injected side and noninjected side of the brain), the global changes in the αSyn content, dopaminergic neuron content, and microglial and astroglial activation were evaluated by western blot method.

2.1.3. Study 3.

This study is focused on whether microglial activation enhance αSyn This study focused on whether increased inflammatory activation enhances the αSyn propagation and whether microglial inhibition decreases the αSyn propagation. This study scheme is shown in Figure 2. At 14 days after the intrastriatal injection of lipopolysaccaride (LPS) or control substance (PBS) with αSyn PFF, the αSyn propagation was compared between the groups. A microglial inhibitor, PLX5622, or PBS was administered for four weeks, two weeks each before and after the intrastriatal αSyn PFF injection. At 7 and 14 dpi, the amount of αSyn accumulation was compared between the PLX5622 group and the control group.

Figure 2. Study 3 schematic
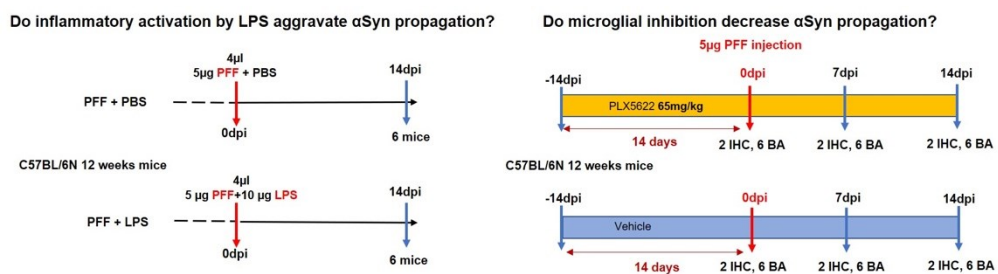
2.2. Method of Research

2.2.1. Preparation of fibrillar αSyn

2.2.1.1. Production of recombinant αSyn monomer [①]

The PD434-SR mouse αSyn vector from Addgene (plasmid #89073, https://www.addgene.org/89073) was amplified in *E. coli* DH5α. The expression vector was transformed into the *E. coli* BL-21 bacteria. The selected single colony was grown in a 2xYT medium supplemented with 100 µg/mL of ampicillin. The growth was monitored and followed by protein induction. The harvested pellet cells were collected and resuspended in distilled water, which was supplemented with 50 µL of saturated $MgCl_2$ and kept at −80°C overnight. Then, the homogenates were boiled at 98°C and centrifuged at 13000 rpm for 20 min. The supernatant was collected, and further dialysis was performed. The αSyn protein sample was placed into 2 L of ice-cold 20 mM Tris-HCl buffer with a pH of 8.0 overnight. Next, the solution was filtered using a 0.2-µm filter; then, the protein was purified using a HiTrap column with buffer A (20 mM Tris-HCl with a pH of 8.0) and buffer B (20 mM Tris-HCl and 1 M NaCl with a pH of 8.0). The eluted fraction containing the αSyn protein was collected and further dialyzed in water at 4°C overnight. Then, the dialyzed protein sample was frozen until completely dry, and the αSyn protein was dissolved in 20 mM Tris-HCl and 150 mM NaCl with a pH of 8.0. Finally, the protein sample was centrifuged at 13000 rpm at 4°C, and the supernatant containing the αSyn was collected and kept at −80°C until further investigation.

2.2.1.2. Generation of αSyn preformed fibril (PFF)

Sigmacote was treated to a siliconized 1.5-mL Eppendorf tube to prevent the surface absorption of the protein. Then, 1 mL of recombinant monomeric αSyn coupled with 10 µL of 5% sodium azide and two small (5 mm) glass beads were added to the tube. The tube was continuously shaken at 800 rpm and 37°C for 10 days using a Thermoshaker. The protein concentration of PFF was measured, and αSyn PFF (2.5 mg/mL) was stored at –80°C before use.

2.2.1.3. Quality assessment of αSyn PFF

[①] This work was done by Phuong Thi Nguyen and Yun Kyoung Lee

Thioflavin T (ThT, Sigma, T3516) assay and transmission electron microscopy (TEM) were used to validate the PFF formation (Fig. 3). The ThT solution (0.0001% in 1 × PBS; 2 μL) and 2 μL of the αSyn PFF and monomer sample were incubated for 5 min in the dark. The fluorescence signal from the αSyn PFFs compared with the monomer was read at an excitation wavelength of 450 ± 10 nm and emission wavelength of 480 ± 30 nm. The difference in the ThT signal between the monomer and PFFs was around 30-fold (Fig. 3b). For the TEM observation, the αSyn PFFs adsorbed onto the grid (carbon grid, TED PELLA) were negatively stained with 2% uranyl acetate solution. The image in Figure 3a was acquired using TEM (JEM1011) at 80 kV. [2]

Figure 3. Validation of αSyn preformed fibril (PFF) using a. transmission electron microscopy (a) and Thioflavin T assay (b)[3]

Scale bar 500nm
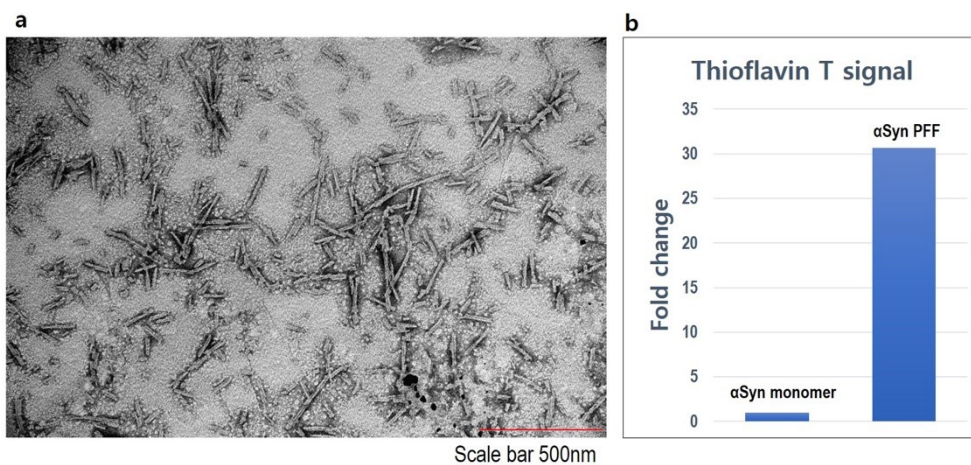
2.2.1.4. Preparation of PFF for surgery

The PFF was taken out from the freezer and melted on ice. ThT assay was performed immediately to confirm the quality of PFF before use. Then, the PFF was sonicated for 10 min at 37°C in an ultrasonic water bath before use to turn PFF into small fragments.

---

[2] TEM was done by Sejin Park
[3] This figure was guoted from a paper published by Young Eun Kim (Preferential microglial activation associated with pathological alpha synuclein transmission)

2.2.2. PD mouse model

2.2.2.1. Mouse husbandry

Young adult wild-type mice (C57BL/6N, male) aged 12 weeks (Young Bio Company, Korea) were used in this study. For the analysis, there were six to nine mice in each experimental group. The number of animals was described in each Figure. All animals were housed at a constant room temperature (RT) with a 12-h light–dark cycle in an animal facility. The beddings and foods were replaced every week until sacrifice. The Animal Research Committee of Hallym University Sacred Heart Hospital approved this study (HMC2019-1-1130-42 and HMC 2020-1-0723-31). All methods were performed in accordance with the relevant guidelines and regulations in the methods section.

2.2.2.2. Intrastriatal injection of αSyn PFF into the striatum

The mice were anesthetized via intraperitoneal injection (i.p.) of avertin solution (240 mg/kg, 0.2 mL/10 g, i.p.) and subcutaneous injection of ketoprofen (0.2 cc of 1%, ketoprofen, s.c.) for pain relief. Toe-pinch maneuver was used to check the status of anesthesia. Haircut and sterilization of the injection site were done. The unilateral intracranial injection of 2 µL of αSyn PFF (same volume of PBSc or monomer αSyn) was performed on one side of the striatum with a speed of 1 µL/min using a stereotaxic instrument. The injection target was the right dorsal striatum with the following coordinates from the bregma: anterior–posterior +0.5 mm, mediolateral −2 mm, and dorsoventral at a depth of −3 to -3.5 mm according to the mouse brain atlas.

2.2.2.3. Sacrifice of the mice and obtaining the brain slices

The mice were anesthetized with an avertin solution and were transcardially perfused with 50 mL of ice-cold 1xPBS, followed by 30 mL of ice-cold 4% paraformaldehyde (PFA). Then, the brain was extracted and fixed in 4% PFA at 4°C overnight. The brains were sectioned in a coronal view using a vibratome at 40-µm thickness, and the cutting speed was 0.055 mm/s. The sections were collected from the olfactory

nerve to the SN, and the sectioned tissues were put in order in a 96-well culture plate. They were stored in 0.05% sodium azide at 4°C until they were used for immunostaining.

2.2.2.4. PLX5622 treatment

For four weeks, the mice were treated with PLX5622 solution (65 mg/kg per day) or PBS by oral gavage. The LPS (5 µg/µL in distilled water, sigma L3129) from *E.coli* O127:B8 was used for intrastriatal injection to induce microglial activation.

2.2.3. Immunofluorescence & immunohistochemistry of the brain tissue

The free-floating tissue sections were washed in 1xPBS for using a shaker for 20 min at RT. Blocking the nonspecific binding by 0.5% Triton X-100 in PBS with normal donkey serum (1:1000) was done on a shaker for 1 h at RT. Then, the brain sections were incubated with primary antibodies overnight. Afterwards, the brain tissues were washed and incubated with secondary antibodies conjugated to Alexa Fluor 488, Alexa Fluor 555, DyLight 488, and DyLight 550 for 3 h. The sections were mounted on a slide with DAPI solution using Vectashield.

Anti-tyrosine hydroxylase (TH) antibody was used to measure the dopaminergic neuronal density; anti-ionized calcium-binding adaptor molecule 1 (Iba1) antibody for microglia, anti-glial fibrillary acidic protein (GFAP) for astrocytes, and anti-phosphorylated Ser129 αSyn antibodies (pαSyn) and anti-αSyn antibodies were used as primary antibodies.

For immunohistochemical staining, the tissues were washed with 1x PBS for 20 min on a shaker; then, endogenous peroxidase blocking was done using 0.3% H_2O_2 for 15 min at RT. To block the nonspecific binding of immunoglobulin, the sections were continuously incubated in 2% BSA and 0.3 % Triton X/PBS for 1 h at RT. The primary antibodies were incubated overnight at 4°C and were further incubated with HRP-conjugated secondary antibodies for 2 h at RT. Then, the brain sections were developed in 1 mL of DAB reagent for 3 min and were immediately transferred to

distilled water. Finally, the tissues were transferred to a coated slide with a mounting solution and were stored at 4°C.

2.2.4. Western blot

The mouse brain was dissected into two parts (PFF-injected side and noninjected side) without the cerebellum. The brain was homogenized in a nonionic detergent-soluble (NP40-soluble fraction) and ionic detergent (NP40-insoluble fraction). The mouse brain was homogenized in a nonionic detergent (10 mM Tris-HCl, pH 7.4, 150 mM NaCl, 5 mM EDTA, 0.5% Nonidet P-40, 1 × phosSTOP, and 1 × protease inhibitor cocktail) and was centrifuged at 12000 rpm for 20 min at 4°C. The supernatant part was the NP40-soluble fraction. Then, the pellet was washed twice with a nonionic lysis buffer and was homogenized with an ionic detergent (10 mM Tris-HCl, pH 7.4, 150 mM NaCl, 5 mM EDTA, 0.5% Nonidet P-40, 1% SDS, 0.5% sodium deoxycholate, 1 × phosSTOP, and 1 × protease inhibitor cocktail); it was incubated on ice for 5 min and was then centrifuged at 12000 rpm for 40 min at 4°C. The resulting supernatant (NP40-insoluble fraction) was collected. The protein concentrations were determined by BCA assay.

The protein samples were treated in a dye solution (5x Laemmli sample buffer) containing 2% SDS and 5% β-mercaptoethanol for 3 min at 100°C. Equal amounts of the protein samples from each group were subjected to 12% SDS-PAGE for 2 h at 80 V. The gel was transferred to a methanol-activated PVDF membrane using a Mini Trans-Blot electrophoretic transfer cell (Bio-Rad) at 250 mA 90 V constant current for 1 h and 30 min using a Model 200/2.0 power supply (Bio-Rad). The membranes were soaked in a Ponceau S solution to visualize the proteins; these were washed thrice with 1x-TBST buffer for 5 min.

For αSyn detection, to increase the detection sensitivity, the transferred membranes were treated with 0.4% PFA in PBS for 30 min at RT, as previously described.[16] After the incubation, the membranes were washed thrice with 1x-TBST for 5 min and were blocked in 5% (w/v) nonfat dry milk for 1 h at RT. Then, the membranes were incubated with primary antibodies (ab212184, ab51253, Abcam) in a blocking buffer at 4°C overnight and were washed thrice with 1x-TBST buffer for 5 min. The

membranes were incubated again with secondary antibodies (HRP conjugate) in a blocking buffer for 1 h at RT. Regarding other proteins, the PFA was not treated.

Finally, protein detections were conducted using an ECL reagent and ChemiDoc MP Imaging System. The quantitative comparisons between the samples on the blots were processed in parallel.

2.2.5. Analysis

2.2.5.1. Imaging and quantification

Fluorescence images were acquired by confocal microscopy (Zeiss Confocal LSM 700 Carl Zeiss) or Olympus BX51 conventional fluorescence microscopy with U-RFL-T power supply equipped with a 1.25x/0.04NA, 4x/0.1NA, 10X/0.3NA, 20X/0.5NA, and 40X/0.75NA objective lens. The images were processed using a Zen, Carl Zeiss, and ImageJ Fiji software. The signal intensity, cell counts, or cell shape were analyzed in the acquired images using the ImageJ software (https://imagej.nih.gov/ij/).

In study 1, all images were taken on the intended area of the brain, which was described in each Figure. All images were taken by confocal microscopy with the same exposure time and contrast. The gray value was used for analysis. In study 2, the DAB images were measured by optical density (OD) using the ImageJ Fiji software. Color deconvolution was applied on the images using the DAB vector function in ImageJ. All parameters in terms of exposure time, contrast, and resolution for image acquisition by fluorescence microscope were set in a similar manner.

Four slices of images of the striatum of each independent mouse was evaluated, one in each PFF-injected striatum and one in noninjected striatum at each time point, by drawing the region of interest to yield eight mean gray values, with a value of 0 and 255 for black and white, respectively. The observed gray level was converted to relative OD using the following formula OD = log (255/mean gray level).

2.2.5.2. Statistical analysis

In this study, the statistical analysis of the data was performed using the Microsoft Excel, IBM SPSS software (version 24.0, IBM Corp., Armonk, NY, USA), or GraphPad Prism version 5 software (https://www.graphpad.com/). The comparison of cell counts, cell body size, rotarod, and wire hang test results at baseline and each dpi was performed using Wilcoxon signed-rank test. The mean value of OD in different groups and the score of the clasping test were compared between the groups using nonparametric ANOVA (Kruskal–Wallis test), followed by post hoc analysis (Dunn's test). A densitometric analysis of the western blot was performed using the Fiji (ImageJ) software, and the final values were compared using nonparametric ANOVA (Kruskal–Wallis test). The results were considered statistically significant if *$p < 0.05$, **$p < 0.01$, and ***$p < 0.001$.

Chapter 3. Results

3.1. Study 1.

3.1.1. The intrastriatal injection of αSyn PFF induced a widespread αSyn propagation in the brain.

At 1 month after the injection of αSyn PFF and PBS on each side of the striatum, diffusely scattered phosphorylated αSyn (pαSyn) accumulation was observed in various brain regions, including the striatum, cortex, and SN, mainly in the PFF-injected side (Fig. 4).

Figure 4. Widespread αSyn propagation and staining in the mouse brain (striatum level) and SN. a. The triangle arrow indicates the injection site of PFF. **b and c**. Higher magnification of αSyn intracellular inclusion. **d**. αSyn inclusion in the SN of PFF-injected and PBS-injected side.[④]

[④] This figure is from same source of footnote 3
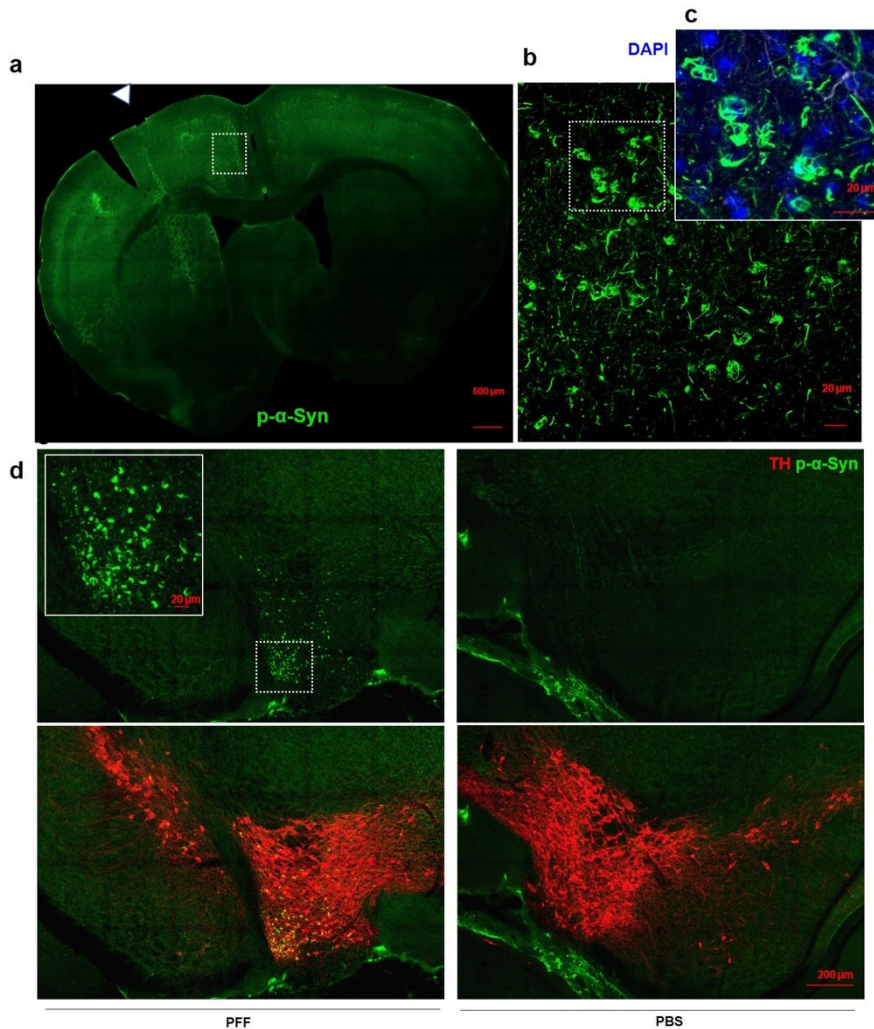
3.1.2. Microglial activation was associated with αSyn propagation in the striatum.

The inflammatory responses were evaluated based on microglia and astroglia in each striatum. In the whole striatum, Iba1-positive microglial cells were observed in the PBS-injected side and PFF-injected side of the striatum (Fig. 5). Because the activated microglia changed their morphology to ameboid form, the cell body size and count of the microglia were evaluated. To avoid immune activation by needle injury or volume effect, stratified images were acquired according to the distance from the injection site, as described in Fig. 5. An increased microglial cell count and microglial cell body size were observed in the PFF-injected striatal area compared

to the PBS-injected striatum (Fig. 5). In particular, microglial soma enlargement was consistently observed in all striatal areas regardless of the distance from the PFF injection site compared to the PBS-injected striatum (Fig. 5). However, the microglial cell count or soma size was not significantly different between the bilateral SN (P > 0.05, last graph of Fig. 6) at the time of evaluation, but the size exhibited an increasing trend in the SN of the PFF side in some cases (P = 0.076).

Figure 5. Evaluation of microglial activation in the striatum[5]

a. Iba1-positive microglial staining of the PFF-injected (PFF) and PBS-injected (PBS) striatum. **b.** Schematic representation of the images acquired from both striata. **c.** Representative image of microglia and αSyn accumulation according to the distance from the injection site. **d.** The microglial cell count was increased in the injection site of both striata; however, the difference between the PFF-injected and PBS-injected striata was not significant at the far periphery of the injection site **e.** The microglial cell body size (average particle size of the microglial cell body) was significantly different between the two striata in all areas. **d–e.** The microglial cell count or average cell body size of was not significantly different in the SN at the time of evaluation ($P = 0.274$ for cell count and $P = 0.076$ for cell body size; t-test). Six mice were used in this study. The cell body size was measured based on the area ($pixel^2$) occupied by the cell body using the average value from each image. Independent t-test or Mann–Whitney U test.
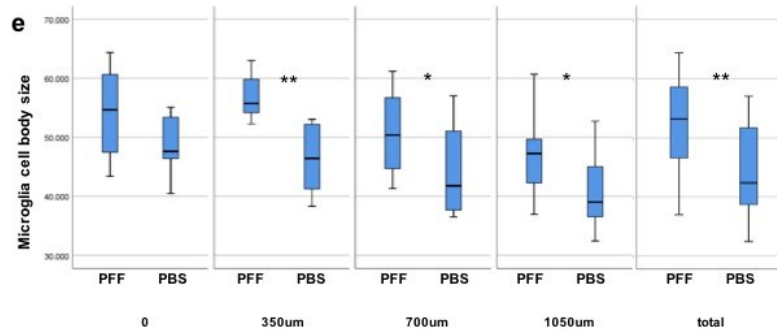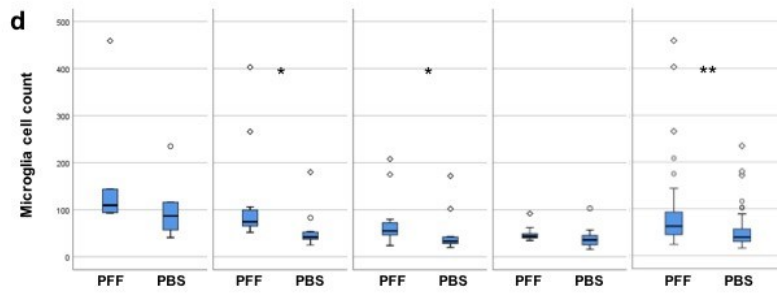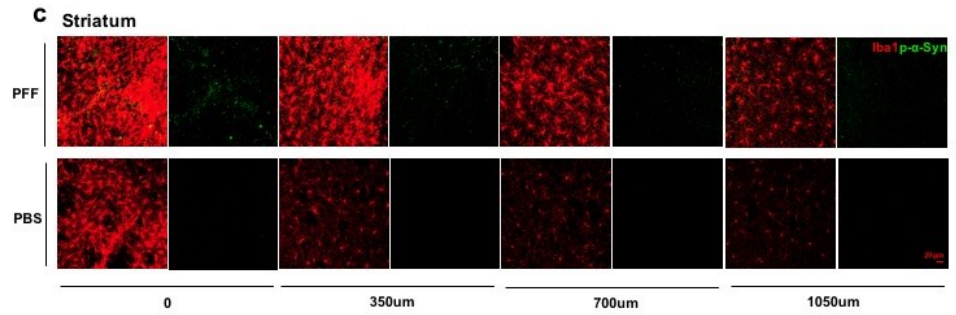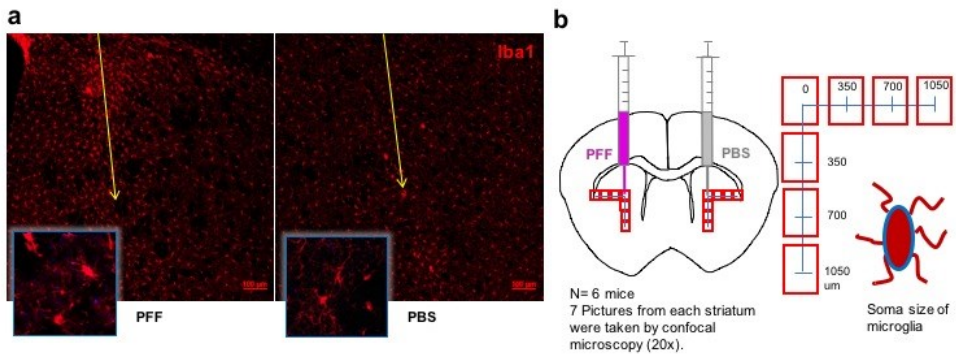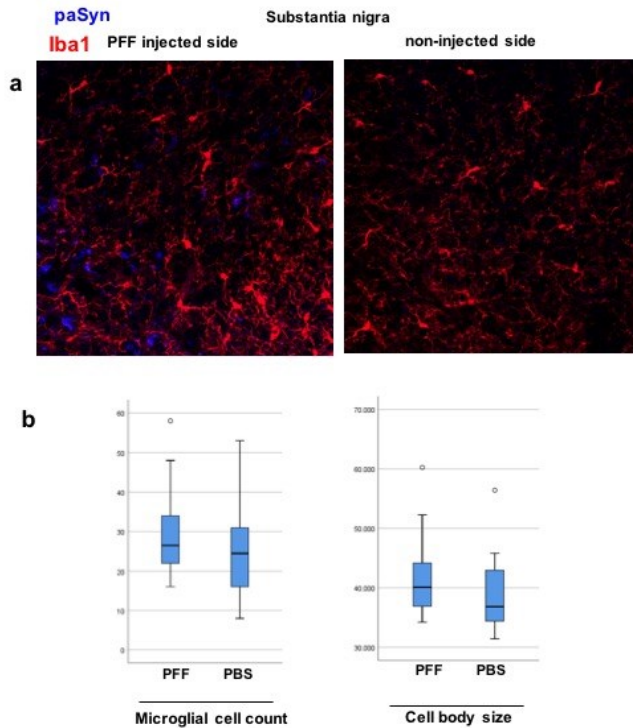

Figure 6. Evaluation of microglial activation in SN. Microglia and pαSyn staining in the SN of PFF-injected side and PBS-injected side (a) and quantification of the cell count and cell body size. (n = 6)


3.1.3. Astroglial activation was not significantly associated with αSyn propagation in the striatum.

Astrocytic activation, as assessed by GFAP staining, was only observed along the injected needle tract in both striata (Fig. 7). Moreover, even though pαSyn aggregates were observed in the periphery of the striatum (to a greater extent in the PFF-injected striatum compared with the PBS-injected striatum), few astrocytic cells were observed (Fig. 7).

Figure 7. Evaluation of astroglial activation in both striata. **a, b.** The GFAP-stained images of the whole striatal area showed astroglial proliferation along the needle injection site (yellow), but it did not indicate the presence of GFAP signal in the periphery of the injection site, regardless of the distance **c.** The mean gray value of the astrocytes (GFAP) increased near the injection site (in both striata), but the difference was not significant in the

periphery (700 and 1050 μm) and SN. Six mice were used in this study.[⑥]
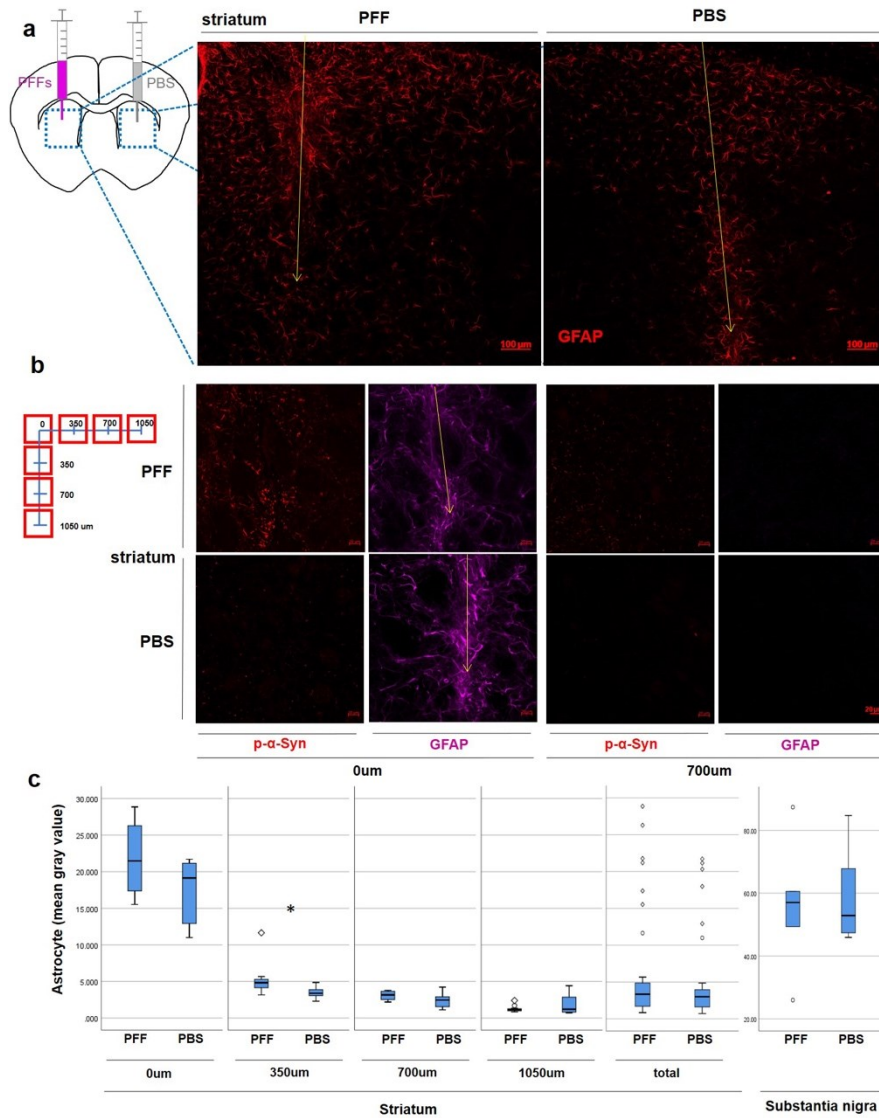
3.2. Study 2.

3.2.1. Intrastriatal injection of αSyn PFF induced the rapid spread of αSyn accumulation in various brain regions with time.

An increased pαSyn accumulation and spreading were progressively observed in various regions, including the striatum, SN, somatosensory cortex, pyriform cortex, amygdala, and hippocampus, during the observation time (Fig 8).
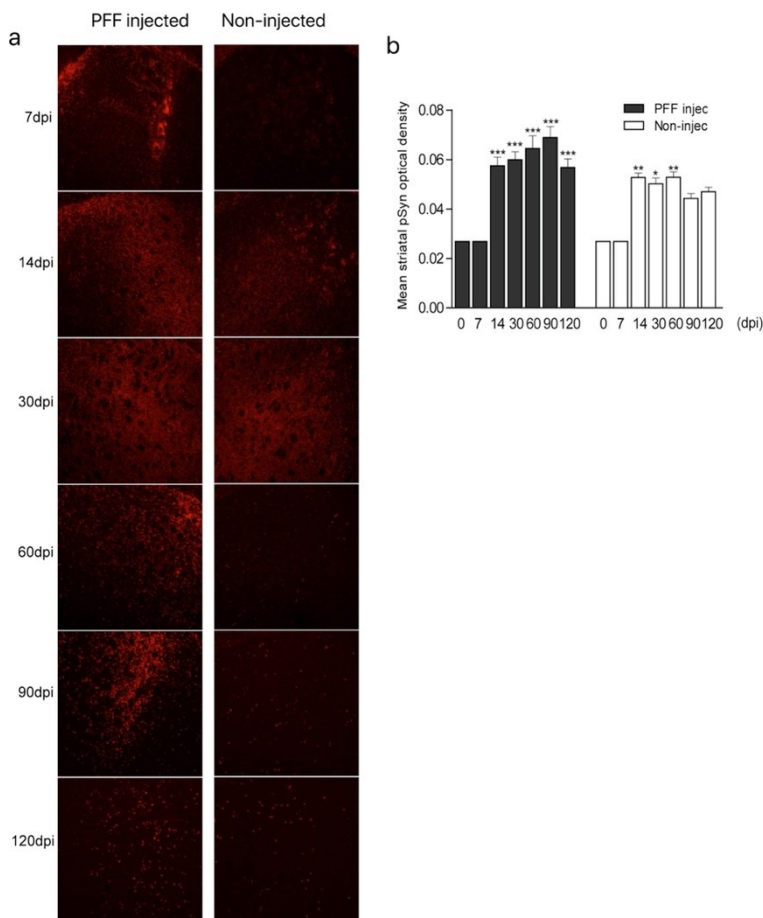
Figure 8. progression of αSyn accumulation in the various brain regions including SN, somatosensory cortex, piriform cortex, amygdala, and hippocampus at different days post injection
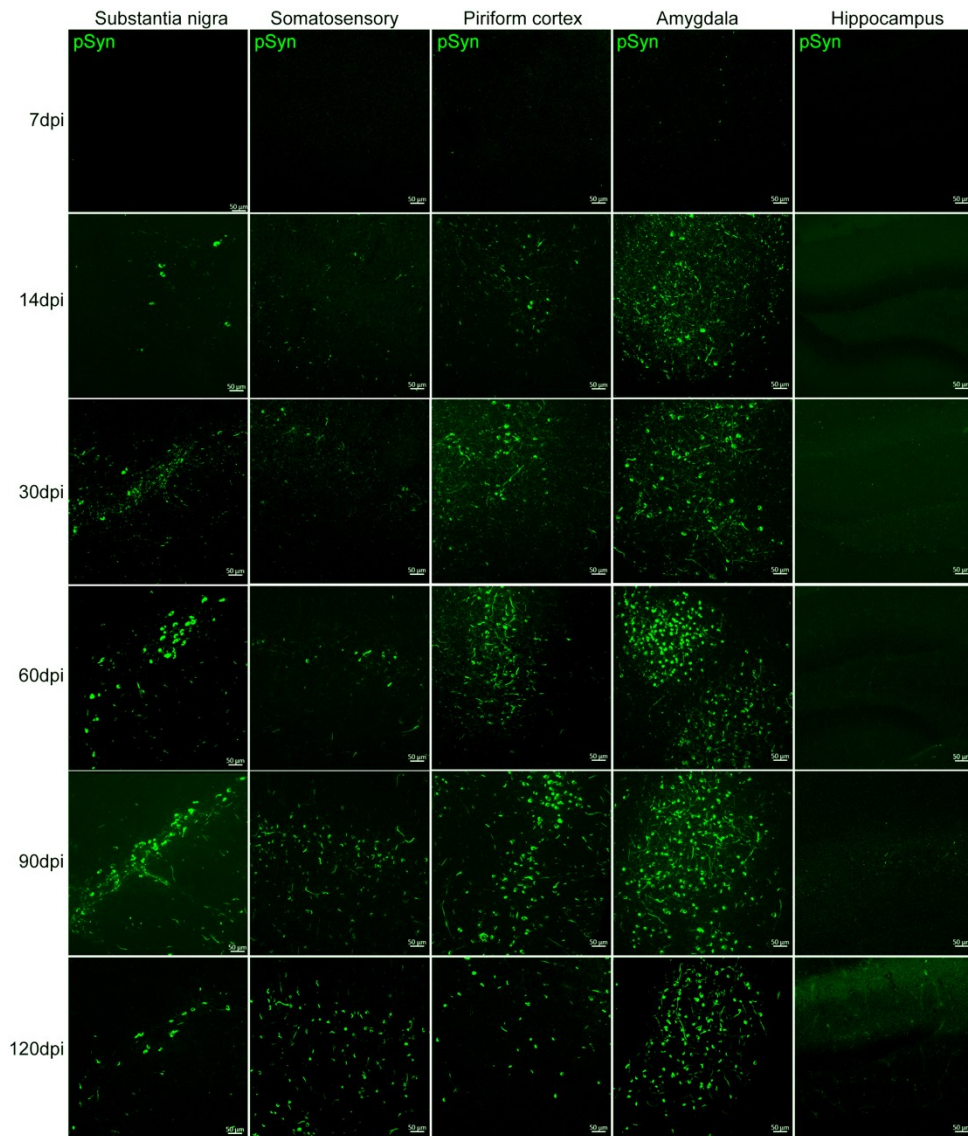
The pαSyn content in the striatum was quantified in the bilateral striatum at each

time points. pαSyn-positive inclusions in the bilateral striatum were observed from 7 dpi, and these increased with time and peaked at around 90 days. (Fig 9). In the noninjected striatum, pαSyn-positive inclusions showed a similar trend at a lesser degree. pαSyn aggregations were not found at baseline (0 dpi without any injection) and were not induced by monomeric αSyn until 120 dpi (Fig 9). pαSyn aggregations were not found at baseline (0 dpi without any injection) and were not induced by monomeric αSyn until 120 dpi (Fig 9).

Figure 9. Changes in pαSyn accumulation in the PFF-injected and noninjected side of the striatum (a) and image quantification (b).[7] Statistical analysis was done in six or seven mice at each time points.

The αSyn contents were measured from NP40-soluble and NP40-insoluble fractions of the brain. The αSyn contents in the soluble fraction increased and peaked at the earliest observation time, 7 dpi, on both sides of the brain. The αSyn in the insoluble fraction slowly increased and peaked at 30 dpi (Fig 10).

Figure 10. αSyn contents from the soluble and insoluble fraction of the brain from each PFF injected and non-injected side. [8]
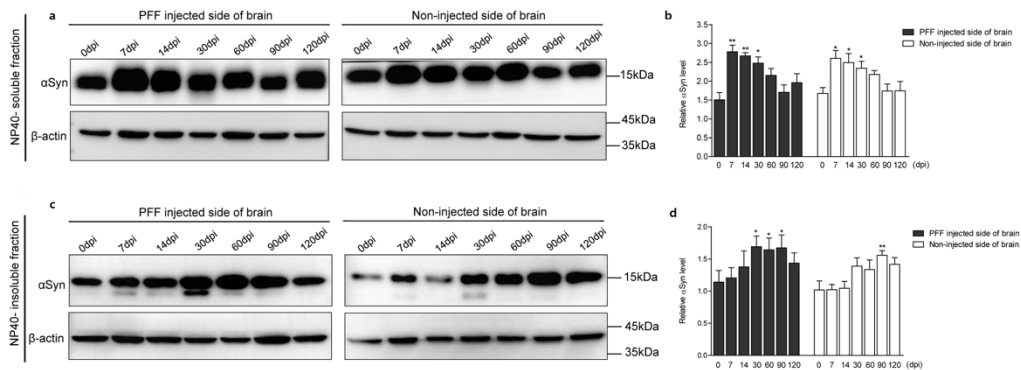
3.2.2. The dopaminergic neurons degenerated during pathological αSyn transmission.

The dopaminergic nerve terminal density in the striatum decreased slowly with time in the PFF-injected striatum (Fig 11a). Compared to the baseline, dopaminergic nerve terminal degeneration was significantly observed at 90 dpi and 120 dpi in the PFF-injected striatum, while it was not statistically significant in the noninjected striatum until after 120 days (Fig 11a).

In the SN of the PFF-injected side, the degeneration of dopaminergic neurons was observed significantly at 60 dpi, but this was not statistically significant in the opposite striatum until 120 dpi (Fig 11b). In the whole brain lysate, the dopaminergic neuronal density tended to decrease in the PFF-injected side of the brain (Fig 11c

---

[8] All works from Figure 10 was done by Thuy Lai Thi and Young Eun Kim.

and d).
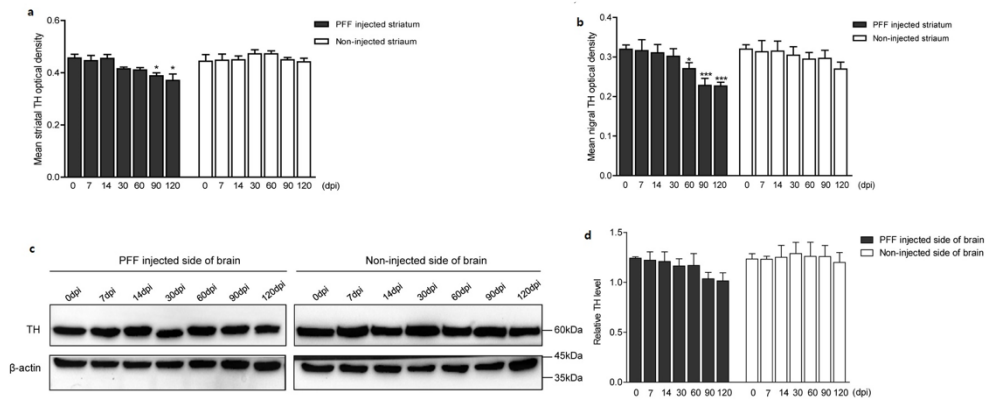
3.2.3. Inflammation showed an early distinct activation in the striatum and whole brain.

The microglial and astrocytic activation were abundantly observed in the striatum of PFF-injected mice at 7 dpi (Fig 11a and d), while it was scanty in the striatum of PBS-injected or monomeric αSyn-injected mice (Fig 12b, c, e, and f).

Figure 13 (top panels). Iba1-positive microglia (A–C) and GFAP-positive astrocyte (D–F) staining. Rows: PFF injected mice at 7dpi (A, D), PBS injected mice at 7dpi (B, E), Mono αSyn injected mice at 7dpi (C, F).
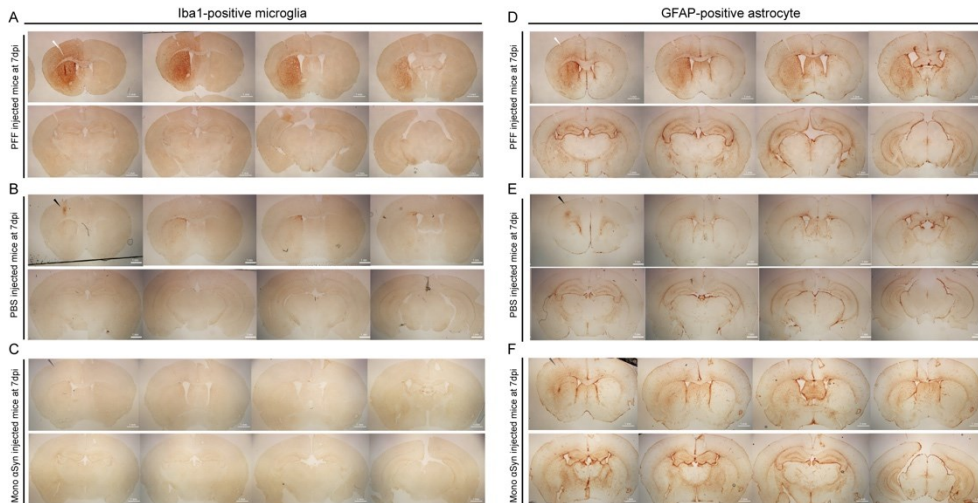
Microglial activation peaked at 7 dpi in both PFF-injected and noninjected striata (Fig 11a). Astrocytic activation increased and peaked at 7 dpi in the PFF-injected striatum, while the opposite striatum did not show a significant increase in astrocytic activation (Fig 13b).

In the whole brain homogenate, the Iba1 level significantly increased at 7 dpi, but it progressively decreased in both sides of the brain (Figs 13c and d). A similar increasing trend in astrocytic response was also observed, but it was not statistically significant (Fig 13e and f).

Figure 13. Microglial and astrocytic activation in the striatum (a and b) and from the whole brain lysate (c and d). a and b quantification graphs are from image analysis of striatum, and c and d are western blot analysis using brain lysate from PFF injected and non-injected side.
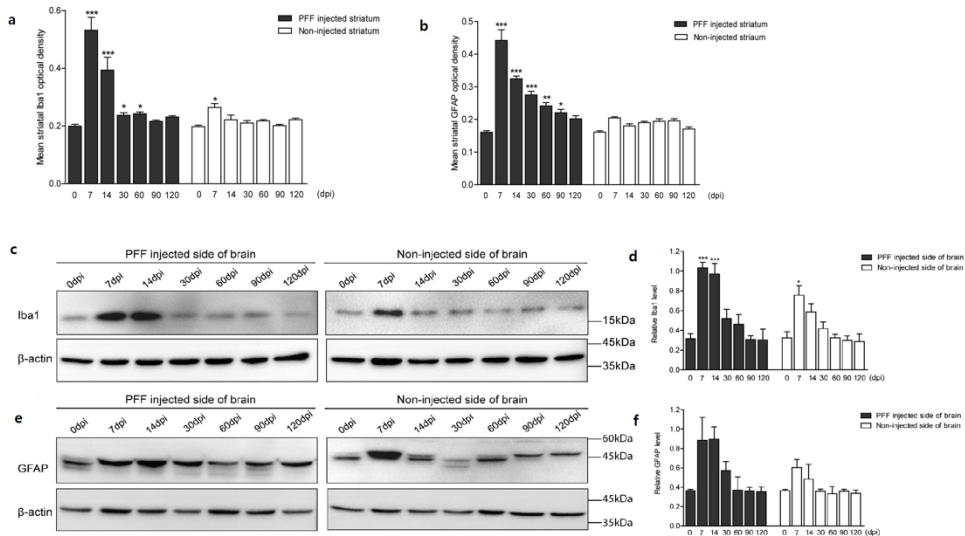
3.2.4. Temporal progression of neuroinflammation, αSyn propagation, and neurodegeneration

Overall, in the striatum of the PFF-injected mice, neuroinflammation started first, followed by pαSyn accumulation and neurodegeneration; however, neurodegeneration was not yet definite in the noninjected striatum (Fig 14a and b). In the whole brain, the inflammatory responses, especially the microglia, considerably increased at first with an increase in the soluble αSyn content. This was followed by the insoluble αSyn content, and dopaminergic neurons tended to decrease lately (Fig 14c and d).

Figure 14. Graph showing the temporal changes in neuroinflammation, αSyn accumulation, and neurodegeneration in the striatum and whole brain.

A PFF injected striatum

B Non-injected striatum

C PFF injected side of whole brain

D Non-injected side of whole brain
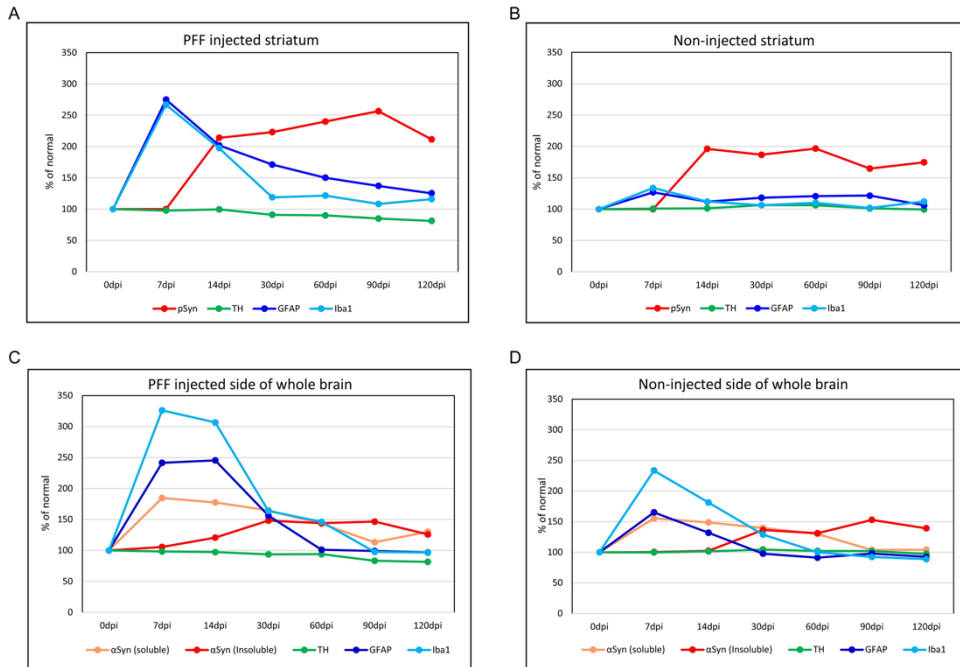
3.3. Study 3

3.3.1. Inflammatory activation by LPS aggravated the αSyn propagation

At 14 days after the PFF injection, with or without LPS, the mouse brain was extracted and evaluated. The pαSyn immunoreactivity was significantly increased in the PFF-injected group with LPS compared with the PFF-only group. (Figure 15)

Figure 15. LPS promoted the αSyn propagation

Iba positive microglial activation was more profound in PFF and LPS-injected mouse brain (b) than in those without LPS (a) at 14 dpi. (a, b, and c) pαSyn immunoreactive inclusion was increased more in PFF and LPS injected mouse brain (e) than in those without LPS (d) at 14 days after injection in striatum (f) and SN (i) (d, e, f, and i) This difference was well-visualized in the somatosensory cortex (SS cortex), hippocampus, and SN (g and h). The graph showed the comparison of mean optical density of pαSyn immunoreactivity in striatum, which is more severe in the LPS injected mice than PBS injected mice.
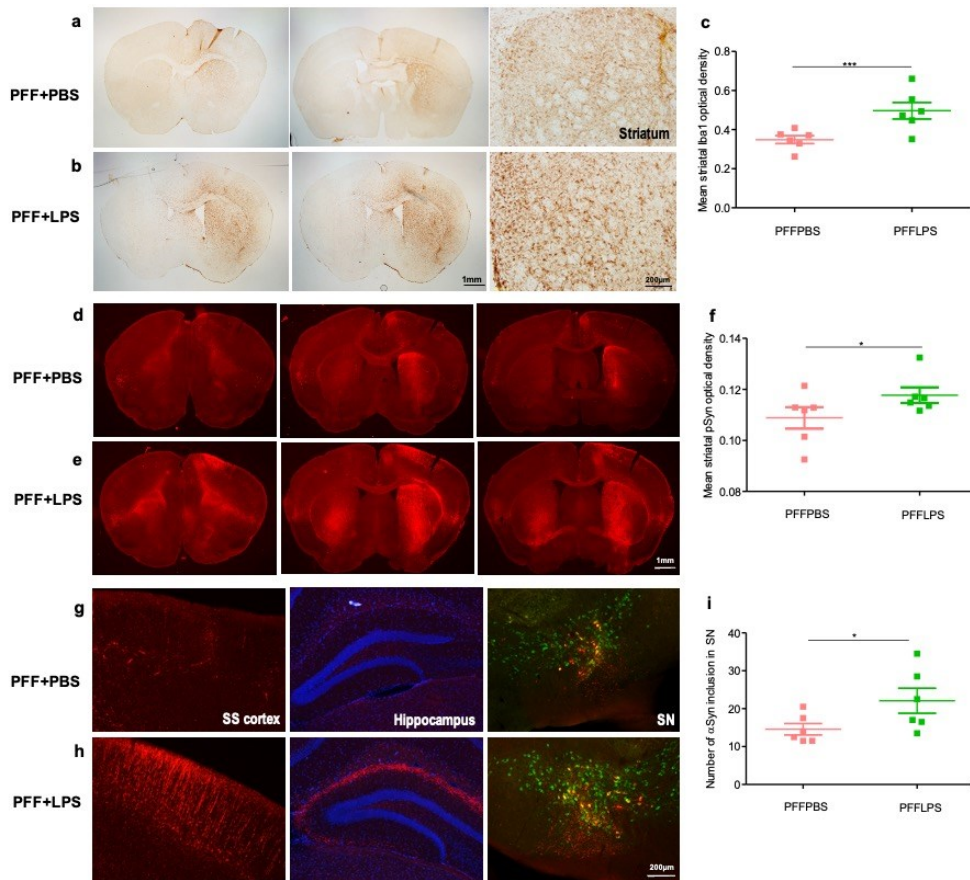
3.3.2. Microglial inhibition by CSF1R inhibitor decreased the αSyn propagation

PLX5622 was administered by oral gavage to reduce the microglial activity for 14 days. In Figure 16, the Iba1-stained microglia were decreased compared with that in vehicle-treated mice at 14 dpi. The αSyn PFF injection showed a significantly less αSyn accumulation in PLX5622-treated mouse brain than in the control brain at 14 dpi (Fig 17).

Figure 16. Microglial activity was decreased in the mouse brain by CSF1R inhibitor. The image shows the Iba1 immunostaining in the mouse brain after the oral gavage of the vehicle or CSF1R inhibitor (PLX5622) for 14 days.
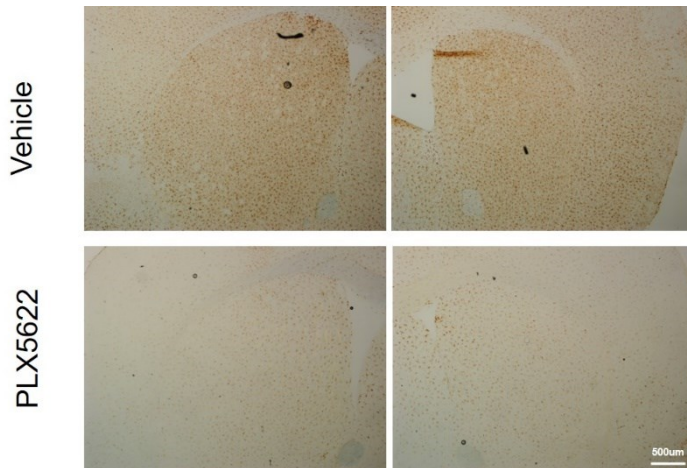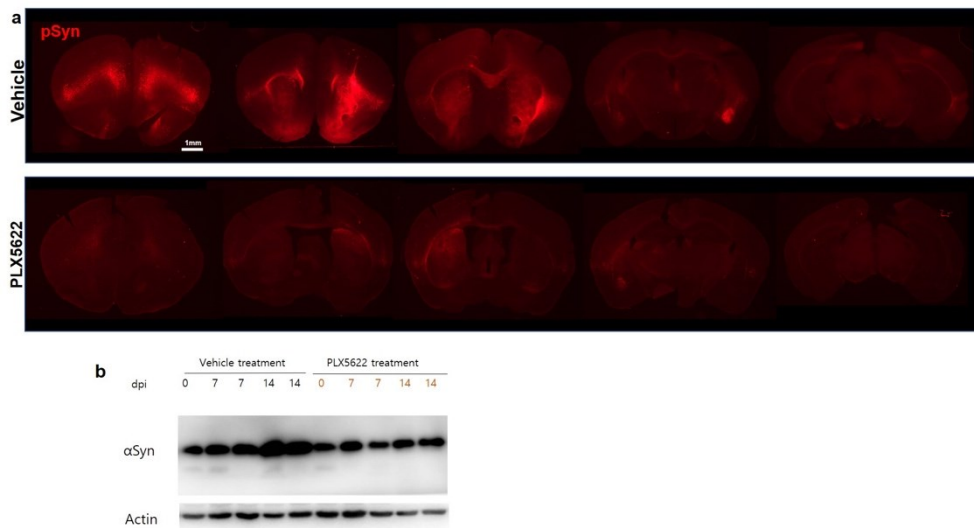
Figure 17. Microglial inhibition suppressed the αSyn propagation.

pαSyn immunoreactive inclusion was less observed in PLX5622 treated mice than in control treated mice. (a) αSyn content was increased in vehicle-treated mice than in PLX5622 treated mouse brain on western blot analysis. (b)

Chapter 4. Discussion

In this study, of the two main CNS inflammatory cells, astrocytes and microglia, microglial activation was associated with αSyn propagation to a greater extent than astroglial activation in the mouse striatum. The peak inflammatory activation was observed earlier than the prominent pathological αSyn accumulation and neurodegeneration. LPS induced inflammatory activation aggravated the αSyn propagation, and the microglial inhibition by a CSF1R inhibitor attenuated the αSyn propagation.

Microglia and astrocytes are the innate immune cells of the CNS. The main action of microglia is to sense and phagocyte pathogens and release cytokines.[17] Astrocytes release various cytokines, maintain the ion balance, provide synaptogenesis, modulate the peripheral immune cells via the blood–brain barrier, and provide a structural defense against pathological changes. [18] In this aspect, microglia may sense the pathologic form of (transmitted or inherently produced) αSyn in their surroundings and become reactive and engulf the pathologic αSyn.[17] In this study, astrocytic proliferation was observed mainly in the regions near the needle injury irrespective of the injected materials, PFF or PBS, even though the astrogliosis in the injected area was more severe in the case of PFF than PBS. However, microglial reactivity was observed in the injected regions and peripheral areas without the physical injury, accompanied by stained pαSyn accumulation. In study 2, even in the noninjected striatum of the PFF-injected mouse, the microglia were activated with αSyn accumulation, while the astrocytes did not show a significant increase. The whole brain homogenate analysis revealed that the microglia showed a prominent activation in the bilateral brain irrespective of the PFF injection side, while astrocytic activation was not statistically significant. This may imply that the spread of pathologic αSyn away from the injection site or on the opposite site of the striatum may induce the activation of the resident microglia. Astrocytic activation was limited to a direct αSyn toxicity and was not activated prominently by the transmitted αSyn compared to microglia. Lee et al. have reported that activated microglia induced the

neuroinflammatory reactive A1 astrocytes, which are neurotoxic phenotypes that rapidly kill neurons [22]. This may imply that microglia may react primarily to pathologic αSyn attack and might determine the fate of astrocytes.

In this aspect, the role of microglia in PD pathogenesis can be the focus of research, rather than astroglia, to further understand the αSyn transmission mechanism and treatment considerations.

From the point of view of inflammation in other PD animal models, the MPTP-injected PD model showed microglial cell activation before astrogliosis or neuronal death.[19] The αSyn-overexpressing transgenic mice also showed an enhanced microglial activation. [20, 21] Duffy et al. reported that microgliosis was induced by Lewy body-like αSyn inclusions in the αSyn PFF-injected mouse model, even though this study did not evaluate the astrocytic activation.[22]

In addition to animal studies, the autopsy study showed that microgliosis was reported more consistently than astrogliosis, similar to this study.[13] Generally, microgliosis has been identified in different PD brain regions, including the SN, putamen, cortex, and limbic system, and it was more frequent around the αSyn-positive Lewy bodies or dying neurons, even though contradictory views have been reported.[23-25] In terms of astrogliosis in postmortem PD brains, astroglial activation has been described in various levels, i.e., marked, mild, or nonexistent astrogliosis. [24, 26-28] Based on these findings, we intended to deactivate the microglia and found that microglial inhibition reduced the αSyn expression or accumulation.

Interestingly, this study found that the level of soluble αSyn rapidly increased after the PFF injection and tended to decrease in both sides of the brain. When the soluble αSyn increased, the insoluble αSyn started to increase. Moreover, a band with a lower molecular weight than the full-length αSyn bands of 15 kDa was observed in the insoluble fraction, and this band was not detected in the soluble fraction. This possibly indicates a truncated form of αSyn. It is known that the truncated form of αSyn is more prone to aggregation than the complete form of αSyn, which accelerated the αSyn aggregation. [29] [30]Altogether, the results suggested that the endogenous αSyn expression increased as soon as the PFF was injected; then, the

increased endogenous αSyn contents changed to an insoluble truncated form and later accumulated.

The temporal relationship between inflammation, pathological αSyn accumulation, and neurodegeneration implied several things. First, fibrillar αSyn injection triggered the inflammation. Because the αSyn monomer or PBS did not induce the prominent inflammation like what fibrillar αSyn did. Second, the peak inflammatory response occurred prior to the accumulation of the pathological form of αSyn. Third, neurodegeneration was the final event, following these two processes. In detail, the administration of fibrillar αSyn induced an increased endogenous αSyn expression and inflammatory activation. With this increased αSyn contents, pathologic accumulation occurred in turn. Recent studies showed the possibility that inflammation can increase simultaneously with or even precede the accumulation of αSyn in PD.[15,31, 32] For this reason, to evaluate whether inflammation contributes to αSyn propagation, the inflammation was artificially increased with an endotoxin, LPS, when αSyn PFF was injected in this study. This study supported that activated inflammation can aggravate the αSyn accumulation and propagation.

In previous literatures, including this study, that used a PFF-injected mouse model, neurodegeneration started later than αSyn transmission, even though the timing of neurodegeneration was different in these studies.[5, 22] In this study, dopaminergic neurodegeneration was observed at 2 months in SN and at 3 months in the striatum of the PFF-injected side after the PFF injection, while noninjected SN showed the trend of dopaminergic nerve fiber loss without statistical significance; moreover, the noninjected striatum did not exhibit the dopaminergic neurodegeneration yet. It means that neurodegeneration occurred last because the noninjected striatum was indirectly affected by transmitted toxic αSyn or less αSyn compared to the PFF-injected striatum. This implied that enough duration for αSyn accumulation or inflammation may be needed for neurodegeneration. In the western blot analysis using the whole brain homogenate, the statistically insignificant decrease in the TH level might be due to the relatively small proportion of dopaminergic neurons in the whole brain lysate.

Practically, it is difficult to observe the exclusive effect of the pathological form of

αSyn on the CNS immune cells in in vivo human studies or based on autopsy data because the human brain tends to have synucleinopathy and mixed pathologies and be affected by uncontrollable factors, such as traumatic injury, aging, infections, and systemic diseases. In addition, because autopsy data are usually from advanced disease stages, the fibrous astroglial substitution of deceased neurons is the likely outcome of the long-term disease course, which may obliterate the effect or the relationship of immune glial cells on the αSyn pathology. Therefore, an αSyn PFF-injected animal model would be helpful in understanding the exclusive relationship between the immune cells and αSyn pathophysiology.

Chapter 6. Conclusion

This study showed that the pathologic fibrillar αSyn induced an early increase in inflammatory response, in especially microglial activation, followed by pathological αSyn accumulation, and thereafter neurodegeneration. The increased inflammation facilitated the pathological αSyn accumulation, and the inhibition of microglia suppressed the αSyn transmission and accumulation. For further understanding, the causal relationship or the detailed underlying molecular mechanism needs to be evaluated for disease modifying therapies.

Bibliography

1.   Kalia LV, Lang AE. Parkinson's disease. Lancet 2015;386:896-912.

2.   Kalia LV, Kalia SK. alpha-Synuclein and Lewy pathology in Parkinson's disease. Curr Opin Neurol 2015;28:375-381.

3.   Singleton AB, Farrer M, Johnson J, et al. alpha-Synuclein locus triplication causes Parkinson's disease. Science 2003;302:841.

4.   Kordower JH, Chu Y, Hauser RA, Freeman TB, Olanow CW. Lewy body-like pathology in long-term embryonic nigral transplants in Parkinson's disease. Nat Med 2008;14:504-506.

5.   Luk KC, Kehm V, Carroll J, et al. Pathological alpha-synuclein transmission initiates Parkinson-like neurodegeneration in nontransgenic mice. Science 2012;338:949-953.

6.   Li X, Sundquist J, Sundquist K. Subsequent risks of Parkinson disease in patients with autoimmune and related disorders: a nationwide epidemiological study from Sweden. Neurodegener Dis 2012;10:277-284.

7.   Wu MC, Xu X, Chen SM, et al. Impact of Sjogren's syndrome on Parkinson's disease: A nationwide case-control study. PLoS One 2017;12:e0175836.

8.   Chang CC, Lin TM, Chang YS, et al. Autoimmune rheumatic diseases and the risk of Parkinson disease: a nationwide population-based cohort study in Taiwan. Ann Med 2018;50:83-90.

9.   Ren L, Yi J, Yang J, Li P, Cheng X, Mao P. Nonsteroidal anti-inflammatory drugs use and risk of Parkinson disease: A dose-response meta-analysis. Medicine (Baltimore) 2018;97:e12172.

10.   Poly TN, Islam MMR, Yang HC, Li YJ. Non-steroidal anti-inflammatory drugs and risk of Parkinson's disease in the elderly population: a meta-analysis. Eur J Clin Pharmacol 2019;75:99-108.

11.   Racette BA, Gross A, Vouri SM, Camacho-Soto A, Willis AW, Searles Nielsen S. Immunosuppressants and risk of Parkinson disease. Ann Clin Transl Neurol 2018;5:870-875.

12.   Tan EK, Chao YX, West A, Chan LL, Poewe W, Jankovic J. Parkinson disease and the immune system - associations, mechanisms and therapeutics. Nat Rev Neurol 2020;16:303-318.

13.   Bruck D, Wenning GK, Stefanova N, Fellner L. Glia and alpha-synuclein in neurodegeneration: A complex interaction. Neurobiol Dis 2016;85:262-274.

14.   Kouli A, Camacho M, Allinson K, Williams-Gray CH. Neuroinflammation and protein pathology in Parkinson's disease dementia. Acta Neuropathol Commun 2020;8:211.

15.   Olanow CW, Savolainen M, Chu Y, Halliday GM, Kordower JH. Temporal evolution of microglia and alpha-synuclein accumulation following foetal grafting in Parkinson's disease. Brain 2019;142:1690-1700.

16.   Sasaki A, Arawaka S, Sato H, Kato T. Sensitive western blotting for detection of endogenous Ser129-phosphorylated alpha-synuclein in intracellular and extracellular spaces. Sci Rep 2015;5:14211.

17.   Hickman S, Izzy S, Sen P, Morsett L, El Khoury J. Microglia in neurodegeneration. Nat Neurosci 2018;21:1359-1369.

18.   Khakh BS, Deneen B. The Emerging Nature of Astrocyte Diversity. Annu Rev Neurosci 2019;42:187-207.

19.   Hirsch EC, Hunot S. Neuroinflammation in Parkinson's disease: a target for neuroprotection? Lancet Neurol 2009;8:382-397.

20.   Su X, Maguire-Zeiss KA, Giuliano R, Prifti L, Venkatesh K, Federoff HJ. Synuclein activates microglia in a model of Parkinson's disease. Neurobiol Aging 2008;29:1690-1701.

21.   miSacino AN, Brooks M, McKinney AB, et al. Brain injection of alpha-synuclein induces multiple proteinopathies, gliosis, and a neuronal injury marker. J Neurosci 2014;34:12368-12378.

22.   Duffy MF, Collier TJ, Patterson JR, et al. Lewy body-like alpha-synuclein inclusions trigger reactive microgliosis prior to nigral degeneration. J Neuroinflammation 2018;15:129.

23.   Imamura K, Hishikawa N, Sawada M, Nagatsu T, Yoshida M, Hashizume Y. Distribution of major histocompatibility complex class II-positive microglia and cytokine profile of Parkinson's disease brains. Acta Neuropathol 2003;106:518-526.

24.   Mirza B, Hadberg H, Thomsen P, Moos T. The absence of reactive astrocytosis is indicative of a unique inflammatory process in Parkinson's disease. Neuroscience 2000;95:425-432.

25.   Mackenzie IR. Activated microglia in dementia with Lewy bodies. Neurology 2000;55:132-134.

26.   Hirsch EC, Hunot S, Hartmann A. Neuroinflammatory processes in Parkinson's disease. Parkinsonism Relat Disord 2005;11 Suppl 1:S9-S15.

27.   Vila M, Jackson-Lewis V, Guegan C, et al. The role of glial cells in Parkinson's disease. Curr Opin Neurol 2001;14:483-489.

28.   Song YJ, Halliday GM, Holton JL, et al. Degeneration in different parkinsonian syndromes relates to astrocyte type and astrocyte protein expression. J Neuropathol Exp Neurol 2009;68:1073-1083.

29.   Groveman BR, Orru CD, Hughson AG, et al. Rapid and ultra-sensitive quantitation of disease-associated alpha-synuclein seeds in brain and cerebrospinal fluid by alphaSyn RT-QuIC. Acta Neuropathol Commun 2018;6:7.

30.   Sorrentino ZA, Giasson BI. The emerging role of α-synuclein truncation in aggregation and disease. Journal of Biological Chemistry 2020;295:10224-10244.

31.   Galiano-Landeira J, Torra A, Vila M, Bové J. CD8 T cell nigral infiltration precedes synucleinopathy in early stages of Parkinson's disease. Brain 2020;143:3717-3733.

32.   Lindestam Arlehamn CS, Dhanwani R, Pham J, et al. α-Synuclein-specific T cell reactivity is associated with preclinical and early Parkinson's disease. Nat Commun 2020;11:1875.

Abstract

Alpha-synuclein (αSyn) propagation and neuroinflammation may play key roles in the pathomechanism of Parkinson's disease (PD), but the association between the involvement of inflammation and pathologic αSyn progression are not yet well understood. In this study, using a PD mouse model injected with intrastriatal αSyn preformed fibril (PFF), the differential responses of the two innate immune cells in the CNS and the temporal evolution of inflammation and neurodegeneration according to αSyn propagation were explored. And it was evaluated whether activated or decreased inflammatory modification affect the αSyn accumulation. This study found that microglial activation was more prominent than astroglial activation in the striatum of the mouse brain after PFF injection. In addition, after the PFF injection, inflammation was activated with an increased soluble αSyn expression, followed by an increased insoluble αSyn accumulation and neurodegeneration. The increased inflammation by endotoxin facilitated the αSyn propagation. In reverse, the inhibition of the microglial activity by a CSF1R inhibitor decreased the αSyn transmission and accumulation. This relationship between the αSyn propagation and inflammation may give a hint on the pathomechanism of PD and on a promising therapeutic target. Its underlying molecular mechanism needs to be evaluated for further understanding.